International Conference on Artificial Reality and Telexistence
Eurographics Symposium on Virtual Environments (2015)
M. Imura, P. Figueroa, and B. Mohler (Editors)

Structural Color Display on Retro-reflective Objects

Toshiyuki Amano[1] and Kensuke Minami[1]

[1]Faculty of Systems Engineering Wakayama University, Japan

Abstract

Structural color display is an illumination projection display technique that can generate a completely altered appearance. It has potential for the visualization of scientific simulation, material perception display, and other applications. This paper investigates how to alternate the directional illumination distribution to display a desired bidirectional reflectance distribution function (BRDF). For the display technique, we modeled the reflection property of retro-reflective coating and lightfield projection using a projector array. Because the overlap creates an illumination error with respect to the desired appearance when we simply project the desired appearance, we propose a projection image optimization method to ensure that we display the desired structural color. We performed an evaluation on the reflective rainbow of an optical disc, and its effectiveness was confirmed through simulation and hardware experiment.

Categories and Subject Descriptors (according to ACM CCS): H.5.1 [Information Interface and Presentation]: Multimedia Information Systems—Artificial, augmented, and virtual realities

1. Introduction

One key issue in projection display is how to change the original appearance of an object to another one using illumination projection. To achieve this goal, researchers have proposed many projection display techniques that use state-of-the-art technology.

Shader Lamps [RWLB01] was a pioneering projection display proposed by Raskar et al. that represented brick texture and shadow animations based on the movement of the sun on a physical model of the Taj Mahal. A virtual photometric environment system [MNS04] made it possible to control lighting directions and the reflection properties of objects. In addition to solid color objects, overlay projection on textured surfaces was also attempted.

The projection display applied for virtual restoration of oil paintings [YHS03] and degenerated ancient clay vessel [ALY08]. Law et al. proposed perceptually based appearance editing [LAS*11]. A high dynamic range display system can show high contrast texture by double modulation, which is a combination of an object's albedo and the overlay projection [BI08]. Shimazu et al. employed a textured object fabricated by a three-dimensional (3D) printer for 3D high dynamic range display [SIS11]. These methods are not limited to solid texture manipulation, but can include human material perception manipulation [OOD10]. Amano implemented a projector camera feedback system that manipulates the human material perception of glossiness and translucency [Ama13]. However, to our best knowledge, there is no work that attempts structural color display using illumination projection.

The projection-based structural color display technique has potential for visualization of scientific simulation, material perception display in art museum, novel attractive interpretation in the theater, and other applications, and we believe it can exploit emerging application field. Most everyday objects have a non-monotonic BRDF and have some structural reflection. The main contribution of this paper is a novel projection display technique to display structural color, and we propose a model for a retro-reflective coating material and an optimization method for images used in lightfield projection.

2. Related Work

The horizontal only parallax auto-stereoscopic 3D display is strongly related to our projection display. The 3D display system, which consists of a projector array [MP04], [YHLJ08] employs two vertically-oriented lenticular lenses and a diffuse screen. The projection image passes through

DOI: 10.2312/egve.20151308

first lenticular lens and focuses on the diffuse screen, then the second lenticular lens redistributes the image in different angular directions. Such a horizontal full-parallax optical system can be constructed by not only back projection but also front projection. The front projection construction is equivalent to lightfield projection display [MP04].

Nagano et al. [NJL*13] proposed an auto-stereoscopic projection display that projects 72 overlay images on a vertically-oriented lenticular screen that has its back painted black. The retro-reflected light is spread to 1 degree horizontally by 60 degrees vertically by the lenticular screen, then the user on the projector side observes the auto-stereoscopic 3D image. The major advantage of projection display is that it is scalable, and hence can fit any screen shape.

Our goal is to achieve a structural color display using projection on an arbitrarily shaped object. The retro-reflection surface, when used with a lightfield projection, projects a directional illumination distribution, and this can be used to display the desired BRDF, not just an auto-stereoscopic 3D display. The 3D display concept that employs a pico-projector array [JJBD11] not only achieves both high spatial resolution and high directional resolution, but also has the capability of creating an arbitrarily shaped display. However, even if the pico-projector could be made smaller, to install multiple projectors in a complex and small object is difficult. Hence, the projection display technique is the best solution for our purpose.

3. Retro-reflection

A retro-reflector reflects light straight back to the light source along the illumination path. This basic feature is well known, and we can find many examples of applications (e.g., road cat's eyes, reflective jackets, and other safety goods.) around us. Several working mechanisms exist for retro-reflection. The corner reflector and cat's eye reflection are widely used in common products. In particular, cat's eye retro-reflection, which uses micro retro-reflective beads, is applicable not only as film tape but also as a spray-on coating material (e.g., PIKALA, Komatsu Process Co., Japan). Hence, we can change the reflection property of a target object to retro-reflection with this spray.

Belour et al. examined three retro-reflection tapes covered with plastic (two from 3M and other from Avery Dennison) and proposed three reflection models that employed a back vector [BPD*14]. The back vector is the direction halfway between the symmetric surface reflection light direction. The authors concluded that the retro-reflection model based on the ABC model [CTL90] combined with the back vector showed good approximation results. However, because a coating material such as PIKALA has no protective plastic coating, we can expect its reflection property to be different from retro-reflection tapes. In addition, the ABC model cannot explain the mechanism for the retro-reflective materials

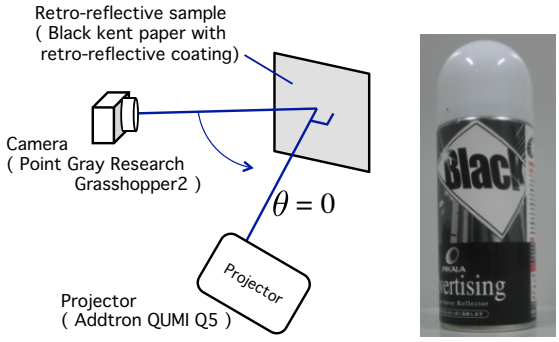

Figure 1: *Left: Experimental setup. We used a piece of black Kent-paper sprayed with a retro-reflective coating. The projector illuminated a white uniform image placed in front of the retro-reflective sample. A linearized response camera observed a fixed point from a constant distance and rotated in the horizontal plane. Then we got a relative irradiance for each view direction. Right: Retro-reflective coating spray can, PIKALA black, Komatsu Process Co., Japan.*

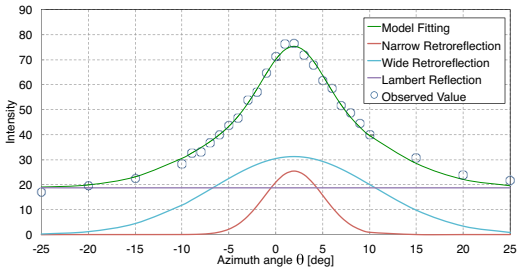

Figure 2: *Observed reflection intensity of the retro-reflective sample. When the camera rotated in the horizontal plane, the intensity shown in the graph (circle marker) was observed at each azimuth angle. The green locus shows the result of our retro-reflection model fit.*

that use micro beads. Therefore, we examined the reflection property of retro-reflective coating material.

Figure 1 shows our experimental setup for measuring the reflection property. The retro-reflective sample was placed in front of a projector and the camera that linearized response measured the reflective illumination of the white projection light at each azimuth angle θ. The blue circles in Figure 2 show the obtained measurements. We can see a peak around $\theta = 2$ degree with a wide distribution elsewhere. This result is different to the features of reflective tape reported in [BPD*14], and we believe the sparse micro bead scattering create the wide dispersion of the distribution and the bright offset of the Lambert reflection component. Therefore, we propose a new retro-reflection model that is composed of two Gaussians for the retro-reflective component

and a constant for the Lambert reflection component as follows:

$$R(\theta,\phi) = k_n exp(-\frac{(\theta-\phi)^2}{\sigma_n^2}) + k_w exp(-\frac{(\theta-\phi)^2}{\sigma_w^2}) + k_l \quad (1)$$

where θ is a viewing direction and ϕ is the direction to the light source (i.e., the projector). Coefficient k_l is the gain of the Lambert reflection, k_w and k_n are the gains of the Gaussians, and σ_w and σ_l are the standard deviation of the two Gaussian reflection components.

In our experiment, we the obtained estimated results $k_n = 25.4, k_w = 31.2, k_l = 18.7, \sigma_n = 4.42, \sigma_w = 12.1$ and a reflection peak position at 1.94 degrees using the Levenberg-Marquardt method. The green locus in Figure 2 indicates this fitting result. The red and aqua colored loci are the two Gaussian components for narrow and wide retro-reflection, and the purple line is the Lambert reflection component.

The coaxial Gaussian mixture model inherits the advantages of good description capability with a finite number of components, and furthermore, the Gaussian function has been employed in many optical models. Because a secondary distribution component exists and its power is strong, the single Gaussian function and Lambert model cannot describe the results of our experiment well. Thus, we added the second term in order to describe the secondary distribution. This second term is a reasonable expression because the secondary distribution of light rays that follow a Gaussian distribution can be written as a Gaussian function with a wider standard deviation.

Because the optical mechanism is common, the model is applicable for other retro-reflective sample which employed micro beads and we expect the model for retro-reflective tape can be described with the addition of a specular reflection component.

4. Lightfield Projection

Our display system consists of seven projectors and a retro-reflective target object. In order to fill the illumination gap along the horizontal direction, we placed projectors at intervals of 5 degrees. This is because the narrow distribution component of the retro-reflective coating has 4.42 degrees of deviation. Thus, the system displays a horizontal light distribution with 30 degrees of directional span and 7 degrees of freedom. Thanks to the overlap of the illumination distributions, a succession transition of the appearance can be displayed. However, this overlapped projection deviates from the desired appearance when we simply project the desired appearance from each projector. Hence, we must optimize the projected image in order to display the correct appearance.

The reflected radiance of the retro-reflective target by the projector array that is observed can be modeled as a summation of the color illumination of all the projections, as

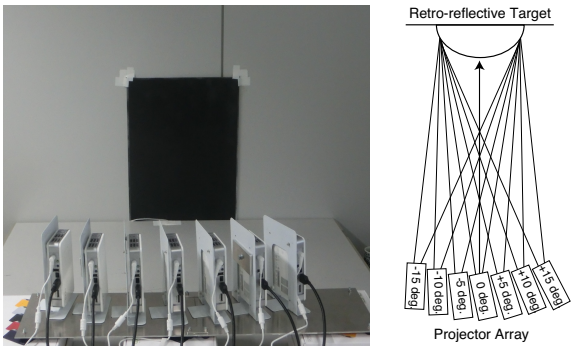

Figure 3: *Our projector array system. Seven projectors are placed in front of the retro-reflective target. The projectors are aligned in the horizontal plane with in 5-degree intervals. Each projector projects a unique image onto the target to display the structural color.*

$$\mathbf{L}(\theta) = \sum_{i=1}^{n} f(\theta,\phi_i)\mathbf{E}_i \quad (2)$$

where $f(\theta,\phi_i)$ is BRDF $f(\theta,\phi_i) = R(\theta,\phi_i)/R(0,0)$, and $\mathbf{E}_i = (E_i^r, E_i^g, E_i^b)^T, i = 1,2,\ldots,n$ is the illuminated power in each channel of the i-th projector that is placed at azimuth angle $\theta = \phi_i$. The optimized projection images $\hat{\mathbf{E}}_1, \hat{\mathbf{E}}_2, ..., \hat{\mathbf{E}}_n$ for each projector can be obtained to solve a non-negative minimization problem

$$\{\hat{\mathbf{E}}_1, \hat{\mathbf{E}}_2, ..., \hat{\mathbf{E}}_n\} = \underset{E_1,E_2,...,E_n}{\arg\min} \sum_{j=1}^{m} ||\mathbf{L}(\theta_j) - \mathbf{I}(\theta_j)||_2, \quad \text{subject to} \quad \mathbf{E}_i \geq \mathbf{0},\ i = 1,2,...,n \quad (3)$$

where $\theta_j, j = 1,2,\ldots,m$ are the sampling points to be minimized. The $\mathbf{I}(\theta_j)$ denote the desired directional color illumination distribution obtained by prior measurement. In the implementation, we obtained pixel correspondences among all projectors then performed optimization for all projection pixels.

5. Experimental Results

For simplicity, we attempted to display the reflective rainbow of an optical disk. Because it is planar shape, we obtained corresponding pixels from each projected image by homography matrices.

In order to decide optimal projection images that display correct appearance at intermediate view points, it requires dense image samples more than the number of projectors. Since we confirmed the illumination smoothly changes along to view direction from our experience (see directional

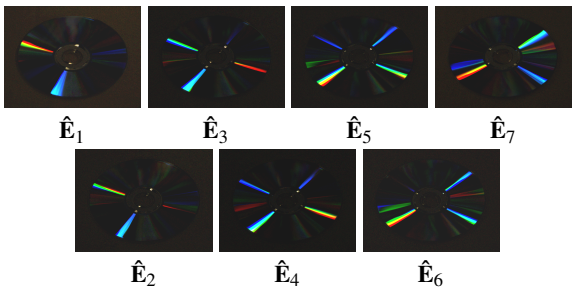

Figure 4: *Optimized projection images obtained by non-negative minimization of the directional illumination distribution error. Images* $\hat{\mathbf{E}}_i, i = 1,2,\ldots,7$ *respectively correspond to projection directions* $\{\phi_i\} = \{-15,-10,-5,0,+5,+10,+15\}$ *degrees.*

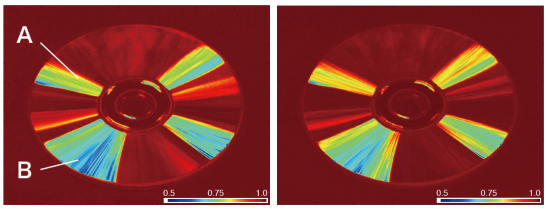

(a) Simple projection (b) Optimized projection

Figure 6: *Normalized correlations expressed by heat map. Because the optimized projection shows a reddish result, we can confirm that the optimized projection displays a more accurate directional illumination distribution.*

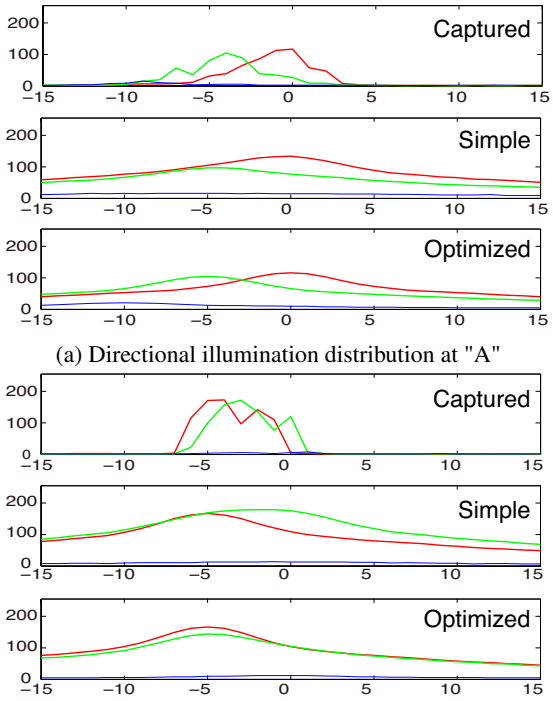

(a) Directional illumination distribution at "A"

(b) Directional illumination distribution at "B"

Figure 7: *The graph shows the illumination distribution according to the view direction (horizontal axis and degree.). Red, green, and blue lines show the intensity of R, G, and B channels. From these results, we can confirm the same trend of directional illumination distribution between the captured images and optimized projection results.*

illumination distribution of captured images in figure 7), we captured 31 images $\mathbf{I}(\theta_j)$ between the azimuth angle of -15 degrees to 15 degrees in 1 degree intervals. These images were obtained by rectification of the captured image with the homography transformation. We then obtained the projection images shown in Figure 4 as a solution of the non-negative minimization.

5.1. Simulation evaluation

Figure 5 shows our simulation results for a simple projection and an optimized projection. The simple projection shows the projection result that used captured images $\mathbf{I}(\theta_i)$ for the projection. The optimized projection used $\hat{\mathbf{E}}_i$. Because the retro-reflection of the retro-reflective coating has a wide angular deviation, both simulation results of the simple projection (second row) and the optimized projection (bottom row) have a wider reflective rainbow than the captured image (top row). However, we can see a spatially smooth transition in the optimized projection result that is similar to the captured images.

In order to evaluate the similarity of the directional illumination distribution, we calculated the normalized correlation of luminance between captured images and simulated results in the angular direction at 31 sampling points. Figure 6 shows the normalized correlations at each spatial position. We can see that the optimized projection shows better reproducibility than a simple projection. Figure 7 shows the detailed illumination distribution at the points "A" and "B." Because retro-reflection has a wide angular distribution and only 7 degrees of freedom can be controlled, both display results have an unsharp response. However, because the color balances of the optimized projection results are similar to the trend seen in the desired directional illumination distribution, we can confirm the projection optimization achieved higher reproducibility.

5.2. Projector array results

We performed hardware experiments to confirm our structural color display concept. Figure 9 shows the appearance of the each view direction. The first row shows images from the simple projection and the second row presents images from the optimized projection. We can see the transition of the reflective rainbow along the view direction. Both appearances are similar, but the results from the simple projection

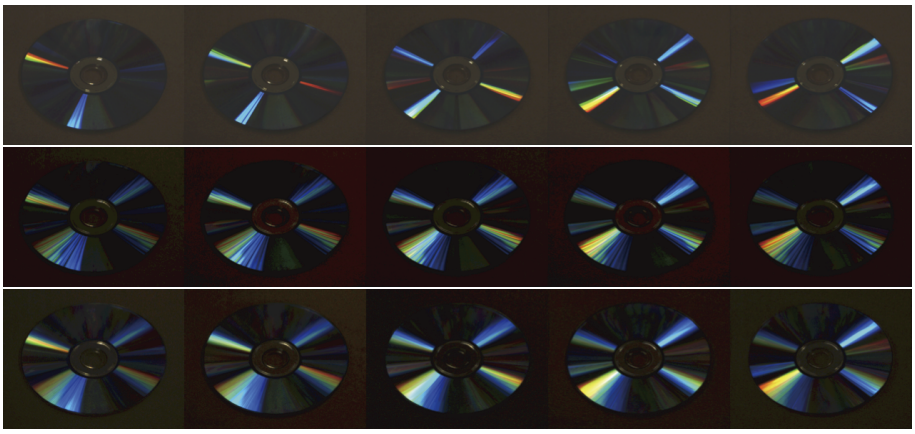

Figure 5: *The top row shows the captured images these are used as ground truth. The middle row and the bottom row show the simulation results of simple projection and optimized projection. From left to right, each column respectively corresponds to a viewing direction of -15, -8, 0, +8, and +15 degrees.*

show a discrete reflective rainbow (e.g., left lower image). This is a similar phenomenon as was observed in our simulation results, and it supports the effectiveness of the optimized projection.

Figure 10 shows the experiment result of morpho butterfly as another sample. As shown in this result, the structural color reflection on the morpho butterfly's wing can be reproduced by the lightfield projection.

6. Discussion

6.1. Optimized projection

The display results using the optimized projection showed a spatially smooth reflective rainbow. Our optimized projection process optimizes the projection power to reproduce a directional illumination distribution. This means its optimization modifies projection power so that the appearance at all intermediate view directions becomes similar to the desired appearance.

When we suppress the over-illumination caused by the overlap of E_1 and E_2 for all view directions, the reshaping of the illumination profile for $\hat{E}_1$ and $\hat{E}_2$, as shown in Figure 8, can be a good solution. With this feathering-like reshaping, we can display a smooth transition of the illumination distribution along with the view direction change as well as smooth transitions. This is the main advantage of the optimized projection.

6.2. Display on a 3D object

The retro-reflective coating can be applied to any object and is not limited by the object's shape. Thus, it is possible to display a directional illumination distribution on a 3D object, as shown in Figure 11. The main problem is how to

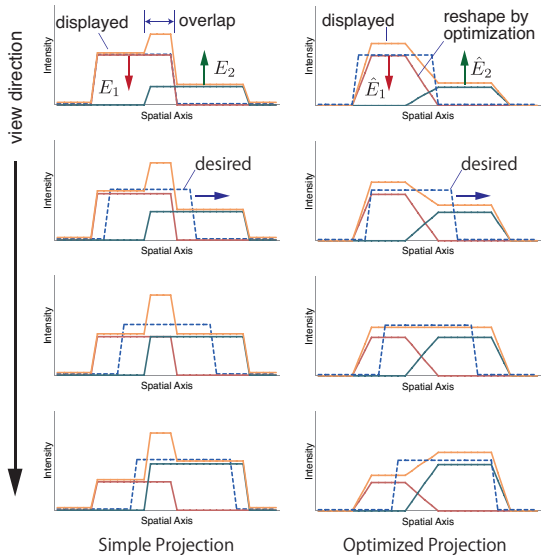

Figure 8: *Projection overlap produces illumination jump when simple projection is used. The projection optimization shapes the illumination distribution into a trapezoid shape.*

obtain pixel correspondences among projectors. As a solution, we can use a gray-code projection on the target object. For instance, we place camera C between two projectors P_1 and P_2 in order to observe each projection as shown in Figure 12. We then obtain two pixel maps $P_1 2C$ and $P_2 2C$ from the camera and projectors with gray-code projections. With an inverse mapping of $P_1 2C$, we can obtain the pixel mapping between the two projectors $P_2 2P_1$. If we obtain all pixel

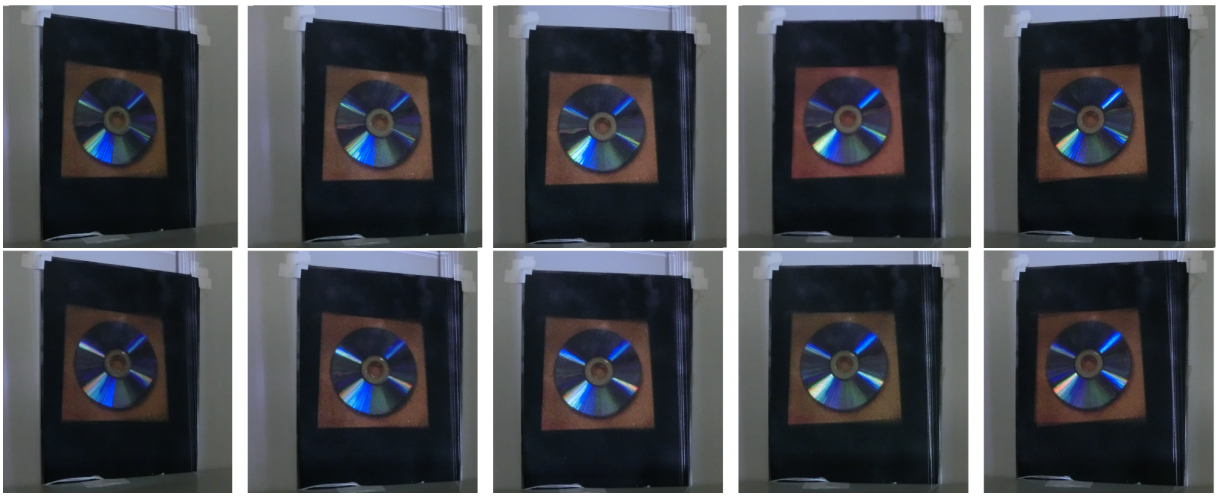

Figure 9: *Hardware experiment results for a simple projection (first row) and the optimized projection (bottom row). The seven images were simultaneously projected by the projector array. Each column shows the appearance observed from the viewing directions of -15, -8, 0, +8, and +15 degrees, respectively.*

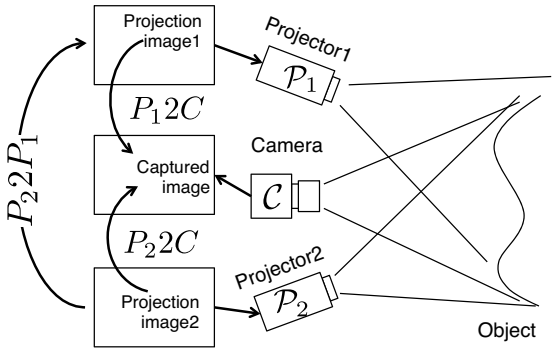

Figure 12: *Projector-to-projector pixel mapping $P_2 2P_1$ can be obtained from two projector-to-camera pixel maps $P_1 2C$ and $P_2 2C$.*

mappings $P_i 2P_j, i \neq j$, it is possible to calculate the optimized projection images for 3D objects.

7. Conclusion

Structural color display is an illumination projection display technique that can display a completely changed appearance on a target object. Therefore, it can be used for the visualization of scientific simulation, material perception display in an art museum, a novel interpretation in the theater, and other applications.

This paper investigated how to alter a directional illumination distribution to display a desired structural color. The basic idea is to use retro-reflective material with a lightfield projection. For this projection display, we proposed a mixed Gaussian model. We then modeled a lightfield projection system and proposed an optimization method for the projection images for structural color representation. The effectiveness of the system was evaluated through simulation and hardware experiments. We would like to apply this technique to 3D objects in our future work.

References

[ALY08] ALIAGA D. G., LAW A. J., YEUNG Y. H.: A virtual restoration stage for real-world objects. *ACM Transactions on Graphics 27*, 5 (Dec. 2008), 1. doi:10.1145/1409060.1409102. 1

[Ama13] AMANO T.: Projection based real-time material appearance manipulation. In *Computer Vision and Pattern Recognition Workshops (CVPRW), 2013 IEEE Conference on* (June 2013), pp. 918–923. doi:10.1109/CVPRW.2013.135. 1

[BI08] BIMBER O., IWAI D.: Superimposing dynamic range. *ACM Transactions on Graphics 27*, 5 (Dec. 2008), 1. doi:10.1145/1409060.1409103. 1

[BPD*14] BELCOUR L., PACANOWSKI R., DELAHAIE M., LAVILLE-GEAY A., EUPHERTE L.: Bidirectional reflectance distribution function measurements and analysis of retroreflective materials. *J. Opt. Soc. Am. A 31*, 12 (Dec 2014), 2561–2572. doi:10.1364/JOSAA.31.002561. 2

[CTL90] CHURCH E. L., TAKACS P. Z., LEONARD T. A.: The prediction of brdfs from surface profile measurements. In *Proc. SPIE* (1990), vol. 1165, pp. 136–150. doi:10.1117/12.962842. 2

[JJBD11] JURIK J., JONES A., BOLAS M., DEBEVEC P.: Prototyping a light field display involving direct observation of a video projector array. *Cvpr 2011 Workshops* (June 2011), 15–20. doi:10.1109/CVPRW.2011.5981693. 2

[LAS*11] LAW A. J., ALIAGA D. G., SAJADI B., MAJUMDER A., PIZLO Z.: Perceptually Based Appearance Modification for Compliant Appearance Editing. *Computer Graphics Forum 30*,

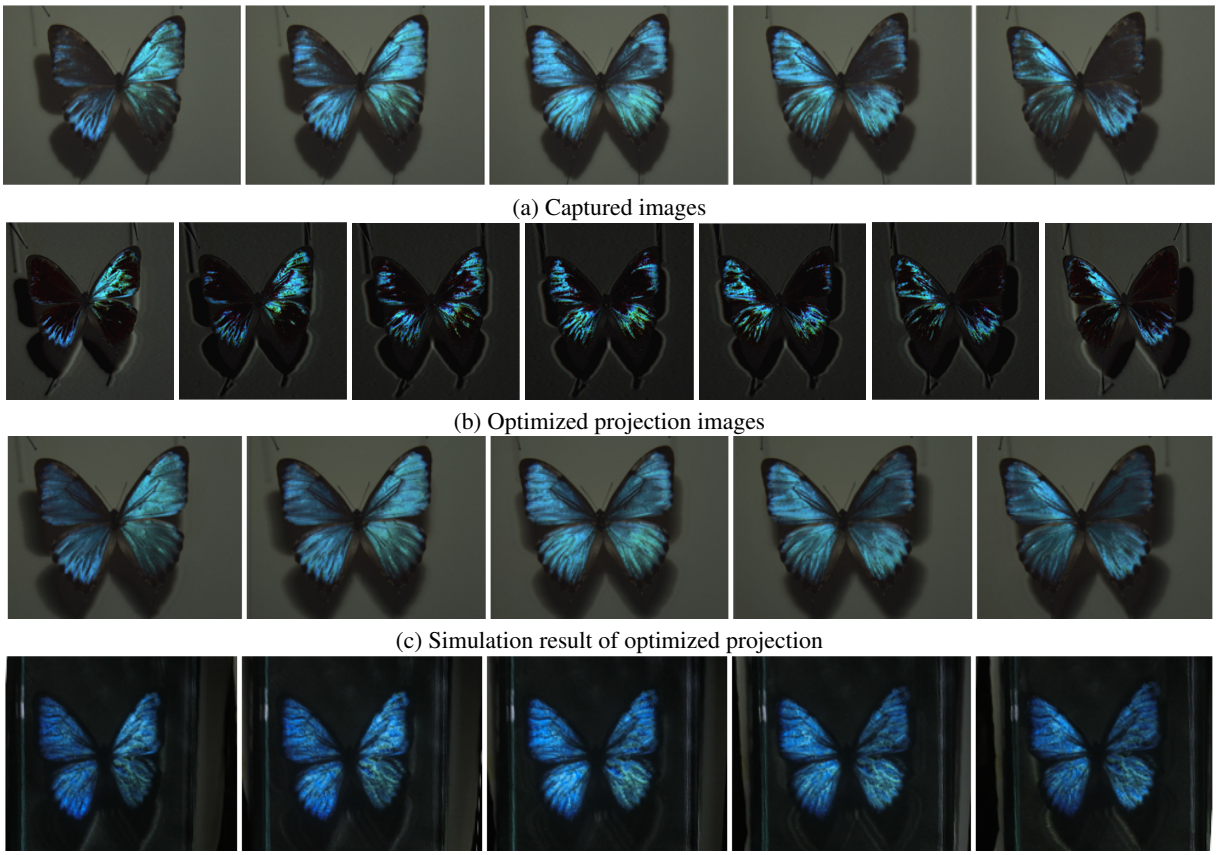

(a) Captured images

(b) Optimized projection images

(c) Simulation result of optimized projection

(d) Hardware experiment result

Figure 10: *Display result of a morpho butterfly. a) We captured 31 images between the azimuth angle of -15 degrees to 15 degrees as a ground truth. Each column shows the captured image at the viewing directions of -15, -8, 0, +8, and +15 degrees. b) Then, we obtained optimized projection images* $\hat{\mathbf{E}}_1, \hat{\mathbf{E}}_2, \ldots, \hat{\mathbf{E}}_7$ *after non-negative minimization. c) The simulation result shows the optimized projection can reproduce structural color of the morpho butterfly on the retro-reflective screen. d) The contrast is decreased, but, we can see a same tendency in hardware experiment result as ground truth.*

Figure 11: *We sprayed the retro-reflective coating on a fabricated 3D object. When the projector array projected various solid colors (rainbow colors) from each projector, we could observe individual colors at different viewing angles.*

8 (Dec. 2011), 2288–2300. doi:10.1111/j.1467-8659.2011.02035.x. 1

[MNS04] MUKAIGAWA Y., NISHIYAMA M., SHAKUNAGA T.: Virtual photometric environment using projector. In *Proceedings of the International Conference on Virtual Systems and Multimedia* (2004), pp. 544–553. 1

[MP04] MATUSIK W., PFISTER H.: 3D TV: a scalable system for real-time acquisition, transmission, and autostereoscopic display of dynamic scenes. *International Conference on Computer Graphics and Interactive Techniques 23*, 3 (2004), 814. doi:10.1145/1186562.1015805. 1, 2

[NJL*13] NAGANO K., JONES A., LIU J., BUSCH J., YU X., BOLAS M., DEBEVEC P.: An autostereoscopic projector ar-

ray optimized for 3D facial display. *ACM SIGGRAPH 2013 Emerging Technologies on - SIGGRAPH '13 28* (2013), 1–1. doi:10.1145/2503368.2503371. 2

[OOD10] OKAZAKI T., OKATANI T., DEGUCHI K.: A Projector-Camera System for High-Quality Synthesis of Virtual Reflectance on Real Object Surfaces. *IPSJ Transactions on Computer Vision and Applications 2* (2010), 71–83. doi:10.2197/ipsjtcva.2.71. 1

[RWLB01] RASKAR R., WELCH G., LOW K.-L., BANDYOPADHYAY D.: Shader lamps: Animating real objects with image-based illumination. *Proceedings of the 12th Eurographics Workshop on Rendering Techniques* (2001), 89–102. 1

[SIS11] SHIMAZU S., IWAI D., SATO K.: 3D high dynamic range display system. *2011 10th IEEE International Symposium on Mixed and Augmented Reality* (Oct. 2011), 235–236. doi:10.1109/ISMAR.2011.6092393. 1

[YHLJ08] YANG R., HUANG X., LI S., JAYNES C.: Toward the light field display: Autostereoscopic rendering via a cluster of projectors. *IEEE Transactions on Visualization and Computer Graphics 14*, 1 (2008), 84–96. doi:10.1109/TVCG.2007.70410. 2

[YHS03] YOSHIDA T., HORII C., SATO K.: A virtual color reconstruction system for real heritage with light projection. In *Proceedings of the International Conference on Virtual Systems and Multimedia 2003* (2003), pp. 161–168. 1